Available online at www.sciencedirect.com
SCIENCE DIRECT®
Journal of Organometallic Chemistry 683 (2003) 269–287
Journal of Organometallic Chemistry
www.elsevier.com/locate/jorganchem

Review

New carbon-rich organometallic architectures based on cyclobutadienecyclopentadienylcobalt and ferrocene modules

Uwe H.F. Bunz [a,b,*]

[a] The School of Chemistry and Biochemistry, Georgia Institute of Technology, Atlanta, GA 30332-0400, USA
[b] Department of Chemistry and Biochemistry, The USC NanoCenter, The University of South Carolina, Columbia, SC 29208, USA

Received 27 February 2003

Dedicated to Professor Lawrence T. Scott

Abstract

This review describes the chemistry of alkynylated cyclobutadiene complexes and alkynylated ferrocenes. These complexes are made by a combination of metalation, formylation and Ohira alkynylation. The transformation of a formyl group into an alkyne is a critical step in these syntheses. The use of a diazophosphonate as the source of a carbon atom is convenient and has allowed for the synthesis of a host of alkynylated π-complexes. Multiply alkynylated ferrocenes and cyclobutadiene(cyclopentadienyl)cobalt complexes are utilized as stepping stone for complex carbon-rich organometallics. Half-wheel, butterfly, and similar structures have been accessed and characterized by single crystal X-ray methods. A ferrocene-fused dehydro[18]annulene decomposes explosively when heated above 200 °C with formation of carbon nanostructures that are bagel- or onion-shaped and that have been characterized by electron microscopy. This account as well describes the synthesis and characterization of organometallic dendrimers and conjugated organometallic polymers.

Keywords: Alkynes; Dehydro[14]annulenes; Dehydro[18]annulenes; Cyclobutadiene complexes; Cobalt; Pd-catalysis; Copper; Carbon-rich materials; Dendrimers; Organometallic polymers

1. Introduction

Carbon-rich and all-carbon materials are fascinating. While until recently only graphite and diamond were known to man, in the last decade other artificial forms of elemental carbon appeared. The fullerenes and carbon nanotubes are these new families of elemental carbon (Fig. 1) [1–6]. Their discovery sparked interest in carbon-rich materials and led to the renaissance of alkyne chemistry. Consequently a plethora of novel carbon-rich compounds has been generated during the last 15 years [7–82].

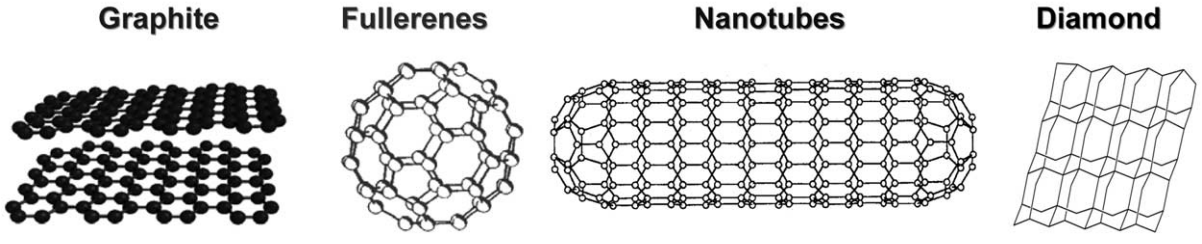

Fig. 1. Known allotropes of carbon.

* Tel.: +1-404-385-1795.
E-mail address: uwe.bunz@chemistry.gatech.edu (U.H.F. Bunz).

0022-328X/03/$ - see front matter © 2003 Elsevier B.V. All rights reserved.
doi:10.1016/j.jorganchem.2003.07.024

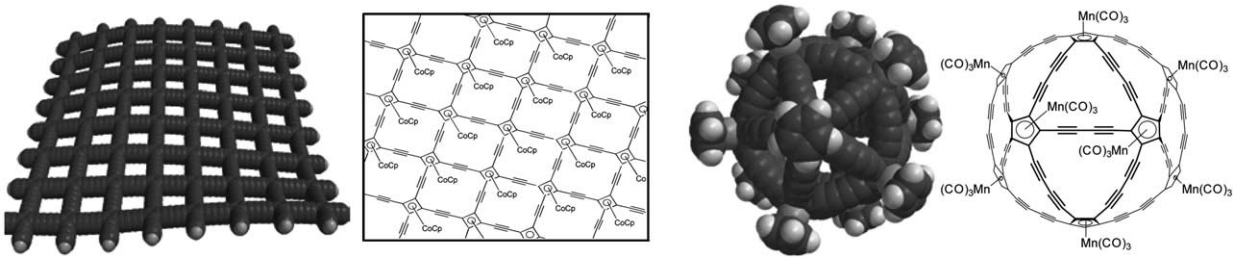

Fig. 2. Hypothetical carbon networks/capsules based on (tetraethynylcyclobutadiene)cyclopentadienylcobalt and on (pentaethynyl)cymantrene.

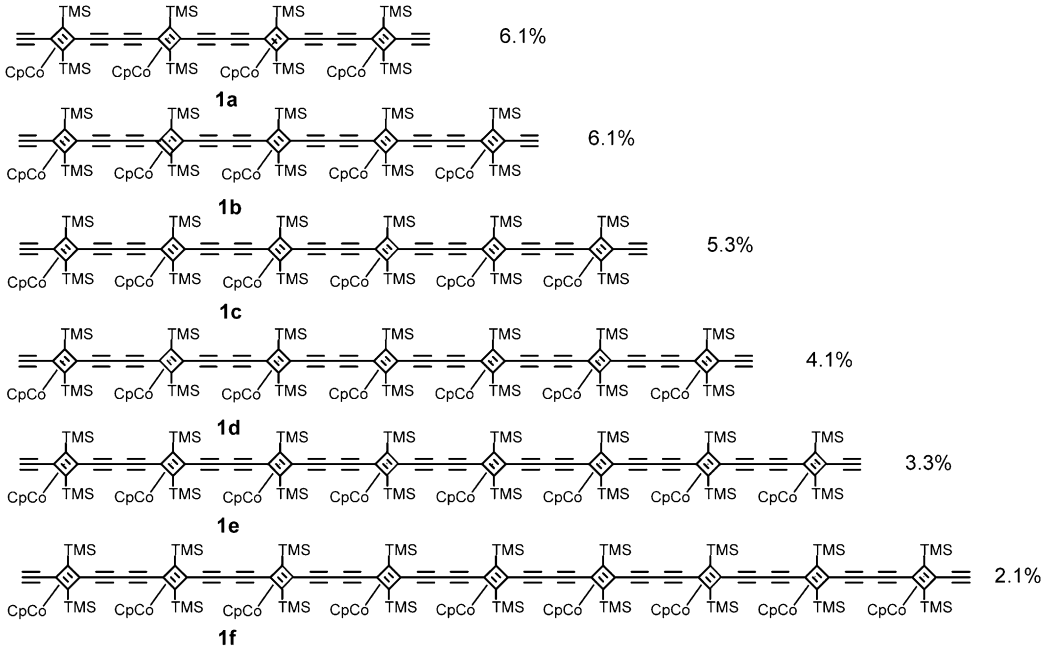

Fig. 3. Increasingly larger oligomers or one-dimensional segments **1a**–**f** out of the organometallic all carbon network shown in Fig. 2. These oligomers have been prepared by the Cu-catalayzed oligomerization of (1,3-diethynyl-2,4-bistrimethylsilylcyclobutadiene)cyclopentadienylcobalt. The percentage numbers on the right side are the isolated yields of the respective oligomer [46].

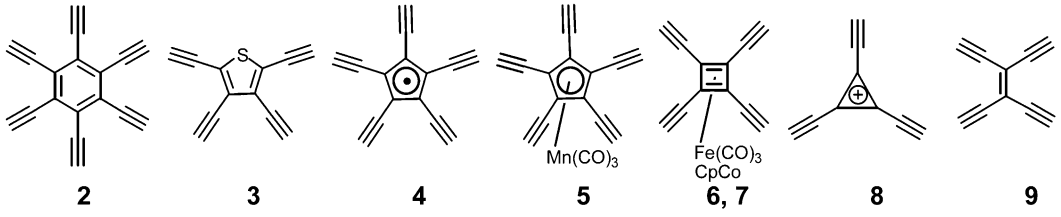

Fig. 4. Simple peralkynylated π-moieties known to date [8–15].

Existing carbon allotropes display five- and six-membered rings exclusively [6]. Neither smaller nor larger rings are present. If one considers the remarkable synthetic flexibility of organic synthesis combined with the propensity of carbon to form double bonds, however, a large number of carbon allotropes featuring different ring sizes can be imagined and might be generated.

If metal-ligated carbon-rich species are included, then the choice of topologies is almost unlimited and the networks/capsules shown in Fig. 2 are conceivable targets. While the organometallic species shown in Fig. 2 should be kinetically stable, their synthesis is not (yet) possible, due to the necessity to form bonds in two dimensions with concomitant control of the ring size. The increase in synthetic effort is formidable if one wishes to progress from one-dimensional polymer/oligomer such as **1a**–**f** [45,46] (Fig. 3) to a network such as depicted in Fig. 2. The extended networks and capsules of Fig. 2 however are useful as a divining rod or

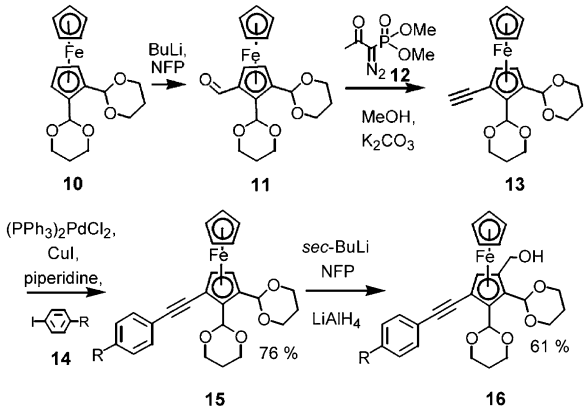

Scheme 1. Metalation, carbonylation, alkynylation strategy for the synthesis of alkynylated ferrocenes. R = methyl or butyl.

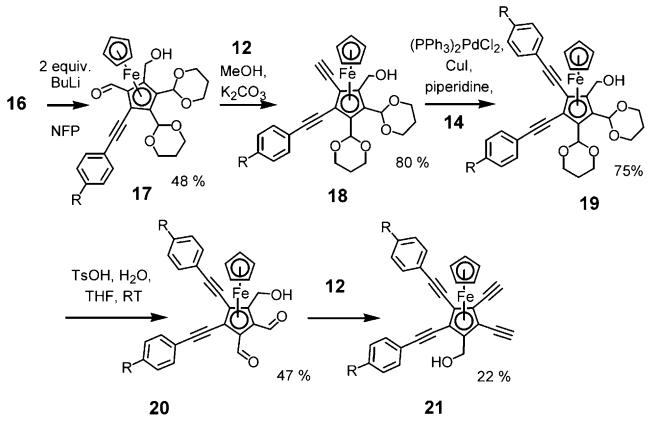

Scheme 2. Metalation, carbonylation, alkynylation strategy for the synthesis of alkynylated ferrocenes. R = methyl or butyl.

blueprint to cut out oligomeric sub-structures that are smaller and therefore accessible by standard synthetic methodology.

In Fig. 4 the known peralkynylated π-perimeters (**2**–**9**) are shown. These structures are good starting points to produce more complex carbon-rich species. Suspiciously absent in this series are pentaethynyl- and decaethynylferrocene, despite the successful synthesis of (pentaethynyl)cyclopentadiene by Rubin and coworkers [43]. and pentapropynylcymatrene by our group [45,47]. In this account the progress in the chemistry of peralkynylated cyclobutadiene complexes, and that of highly alkynylated ferrocenes is presented.

2. Directed metalation, a reliable way to multiply alkynylated π-complexes of cobalt and iron: pentaethynylferrocene

While the (pentaethynyl)cyclopentadienyl anion and radical have been prepared by Rubin and coworkers [43] and pentapropynylcymantrene [45,47] has been reported, pentaethynylferrocene is not known. What is the reason for this sorry state of the affairs? The reaction of the peralkynylated cyclopentadienyl anion with $FeCl_2$ did not lead to decaethynylferrocene but to elemental iron and the (surprisingly stable) peralkynyl–cyclopentadienyl radical. On the other hand, attempts by Michl and coworkers [56] and in our group to alkynylate (pentaiodocyclopentadienyl)(tetraphenylcyclobutadiene)cobalt utilizing a Heck–Cassar–Sonogashira–Hagihara reaction [57–62] were unsuccessful perhaps due to the large steric hindrance that is exerted by the cobalt(tetraphenylcyclobutadiene) fragment. The pentaiodide is simply unreactive to the conditions of the coupling reaction. With these complications in mind, a different, step-by-step 'merry go round' approach to pentaethynylferrocene derivatives **23** was developed [50].

Starting from the bisketal **10**, metalation with BuLi in THF and reaction with *N*-formylpiperidine (NFP) furnished the ferrocene derivative **11** (Scheme 1). The free carbonyl group was transformed into an alkyne by the Ohira–Taber method utilizing the diazophosphonate **12** [63–66]. The alkyne **13** was protected as a benzene derivative (**15**) by a Pd-catalyzed coupling to **14a**. Metalation of **15** was followed by workup with NFP. Subsequent reduction with $LiAlH_4$ in one pot gave the tetrasubstituted ferrocene derivative **16**. The hydroxymethyl group is necessary to perform the next *ortho*-lithiation step. A third metalation was carried out, and reaction with NFP accessed the pentasubstituted ferrocene **17** (Schemes 1 and 2). The aldehyde gave the free alkyne **18**. The alkyne was protected before the two ketal groups were cleaved by *para*-toluenesulfonic acid. The Ohira–Taber reagent then converted **20** into **21**.

The final transformation of the ferrocenemethanol derivative **21** into the pentaethynylferrocene **23** and its dimer **24** is shown in Scheme 3. Airless Marko oxidation [67] of **22** is followed by Ohira alkynylation to give **23a**. To make **23a** symmetric, a Sonogashira coupling was utilized in the last step. In this reaction a 1: 2 mixture of the expected pentaethynylferrocene **23b** and its butadiyne bridged dimer **24** was obtained; **24** must have formed by the oxidative dimerization of **23a** under the employed reaction conditions. Such high-yielding dimerization processes are somewhat unusual but can occur in Sonogashira couplings. They have been discussed by Marder and coworkers [60,61]. Both compounds **23b** and **24** were fully characterized. Unfortunately it was not possible to grow sufficiently large crystals to perform an X-ray analysis [50].

With the experience gathered from the synthesis of **23** a solution phase route to tetraethynylated cyclopetadienylcobalt-stabilized cyclobutadiene complexes could be developed. (Tetraethynylcyclobutadiene)cyclopentadienylcobalt had been obtained by a gas phase pyrolysis

route, significantly restricting the amount of material that could be made [48]. Scheme 4 shows the solution-phase approach [51,52]. Dimerization of the ketal **25** utilizing $CpCo(CO)_2$ (**26**) furnished the desired bis-ketalized cyclobutadiene complexes **27** and **28** after desilylation with tetramethylammonium fluoride. Metalation of **28** and work-up with dimethylformamide (DMF) gave **29**. An Ohira alkynylation followed by treatment with LDA and trimethylsilyl chloride rendered **30**. Protection of the terminal alkyne was necessary for the second metalation of the cyclobutadiene ring to occur smoothly. Repetition of the synthetic sequence on **30** followed by desilylation furnished the 1,3-diethynylated bisketal **31**. Pd-catalyzed reaction with 1-iodo-4-*tert*-butylbenzene (**14c**) protected the terminal alkynes from further deprotonation and other side reactions. Subsequent deketalization of **32a** proceeded smoothly. Without isolation **12** transformed the bisaldehyde **32b** into the tetraalkyne **33**. The compound **33** was characterized by a single-crystal X-ray structure that confirmed the stereochemistry of the cyclobutadiene ring obtained in the dimerization of the ketal **25**. This metalation-functionalited pattern has been utilized in the synthesis of more complex cyclobutadiene(cyclopentadienyl)cobalt-based carbon-rich objects (vide infra). While Scheme 4 shows the preparation of the mutually *para*-tetrasubstituted cyclobutadiene complex **33**, the use of the *ortho*-bisketal **27** proceeds smoothly to give (tetraethynyl)cyclobutadiene complexes of the *ortho*-regiochemistry (vide infra).

The results presented herein demonstrate that metalation-functionalization sequences constitute a general and powerful way to make perethynylated cyclobutadiene complexes and ferrocenes by a stepwise 'merry-go-round' approach.

3. Organometallic dehydroannulenes: more aromatic than benzene?

Benzene, the epitome of aromaticity! It was the first compound to exhibit this phenomenon [68–71]. The special properties of benzene are related to Hückel's rule which states that a cyclic conjugated ring containing $(4n+2)$ π-electrons is particularly stable, i.e. 'aromatic'. This concept was applied to almost all cyclic unsaturated compounds. Aromaticity is—as expected—not restricted to benzene but includes all monocyclic $(4n+2)$ annulenes and dehydroannulenes.

An interesting case is a $(4n+2)$ moiety ligated to a metal center or to an organometallic fragment such as depicted in **38** and **41**. The question arises whether the cyclopentadienyl rings in ferrocene derivatives and in ferrocene itself are aromatic and if they are, will they be more or less so than benzene? To perform a meaningful comparison, a dip-stick for aromaticity would be necessary. Typical indicators of aromaticity are the ring current effect on protons attached to the perimeter as measured by their ^{1}H-NMR shifts and quantum chemical NICS calculations [69]. In the case of ferrocene neither of the two methods gives a good measure of its aromaticity, because both values are distorted by the influence of the sandwiched iron atom. Consequently a more remote way of measuring the aromaticity of the cyclopentadienyl-rings in ferrocene is desirable.

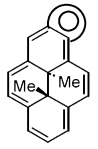

34
Formula block

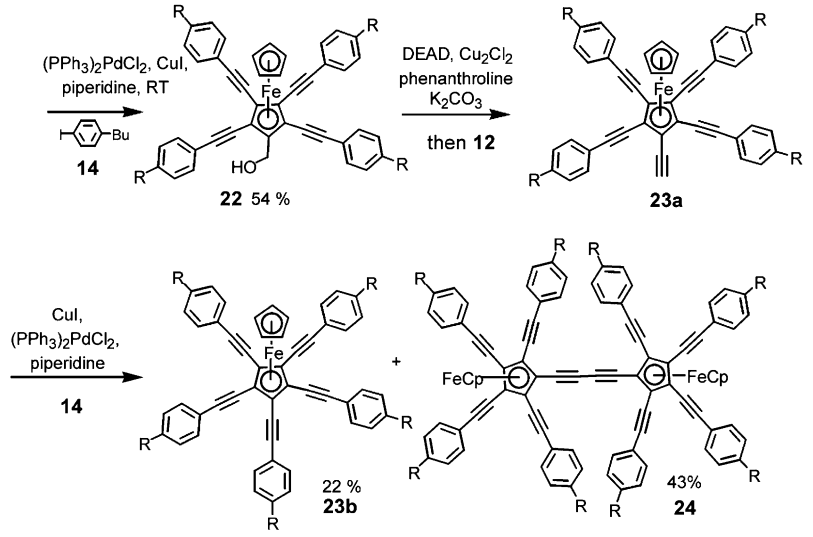

Scheme 3. Synthesis of pentaethynylferrocene **23** and its butadiyne bridged dimer **24**. R = methyl or butyl.

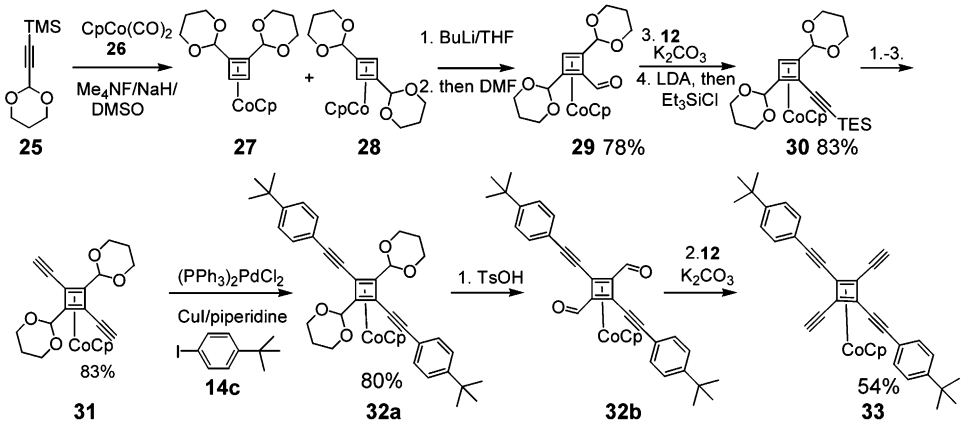

Scheme 4. Solution phase synthesis of a tetraalkynylated cyclobutadiene complex.

Mitchell and coworkers [70,71] suggest dimethyldihydropyrene **34** as a sensitive probe for aromaticity. Upon annelating an aromatic moiety to **34** Mitchell observed shift changes in the ^{1}H-NMR spectra of the attached methyl groups, i.e. the aromaticity change of a reporter is utilized to determine the relative aromaticity of the blue colored unit. The use of **34** as reporter is not imperative. *Any* aromatic unit would suffice. For simplicity of synthesis it was decided to explore the aromaticity of ferrocene by the attachment of an octadehydro[14]annulene. A series of cyclopentano-, benzo-, ferroceno- and cyclobutadieno-fused dehydro[14]annulenes (Schemes 5 and 6) was prepared by a combination of Pd- and Cu-catalyzed reactions [73–77].

The proton NMR spectra of both the open precursors **42**–**45** as well as those of the closed cycles **38**, **41**, **46** and **47** are instructive (Scheme 6). By closing the ring we can observe the effect of the fusion of a π-system onto the aromatic octadehydro[14]annulene. Octadehydro[14]annulene (**47**), the reference system, is aromatic and shows proton shifts of $\delta = 7.24$ and 7.78. Upon attachment of benzene the vinyl protons of the dehydroannulene (**46**) are shifted upfield relative to those of **47** due to the decrease/interruption of the aromaticity of the large ring by the (aromatic) benzene unit.

If ferrocene is annelated to the dehydro[14]annulene instead of benzene, resulting in **41**, the vinylic protons are shifted even more upfield, implying that the localizing power of the cyclopentadienyl ring in ferrocene is larger than that of benzene. The aromaticity of the cyclopentadienyl-ring must be substantial and at least by this measure exceeds that of benzene. The same experiment in the case of the (cyclobutadiene)cyclopentadienylcobalt fused dehydroannulene **38** shows an even larger upfield shift in the vinyl protons Further experiments and calculations will be necessary to either reject or support the somewhat counterintuitive notion that cyclopentadienyl rings and cyclobutadiene rings, when complexed to organometallic fragments, are more aromatic than benzene.

4. Organometallic dehydroannulenes: an explosive access to novel carbon nanostructures [77]

A series of organometallic dehydroannulenes was prepared and crystallographically characterized as shown in Fig. 5. While these organometallic dehydroannulene topologies were previously unknown, and their structures are esthetically pleasing, they are not parti-

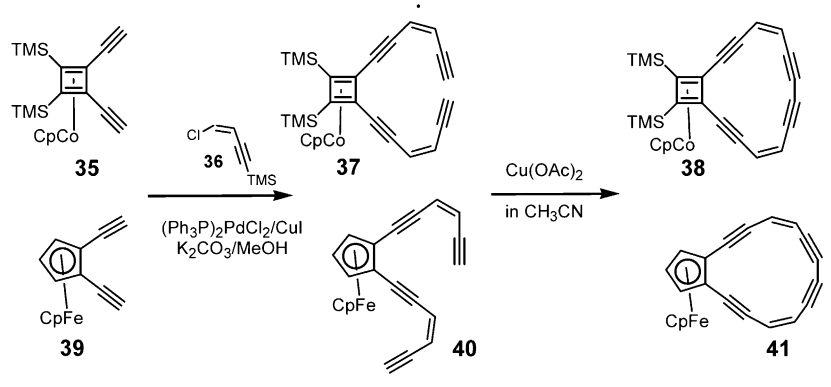

Scheme 5. Synthesis of organometallic dehydroannulenes.

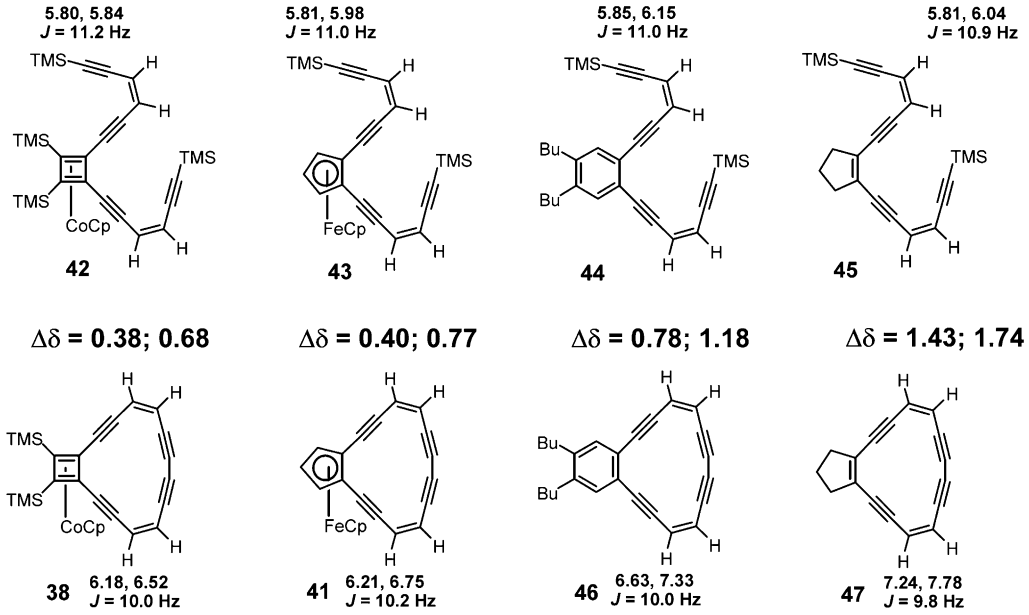

Scheme 6. Comparison of the ^{1}H-NMR spectra of fused dehydro[14]annulenes.

cularly interesting with respect to their thermal solid state reactivity. The smaller dehydroannulenes are stable above 250 °C while the larger ones do undergo a solid-state transformation—but only to form amorphous carbon black according to transmission electron microscopy. That result was somewhat disappointing, because Vollhardt et al. had shown that **50**–**52** formed well-developed carbon nano structures upon pyrolysis [31,32].

One of the cycles that was scrutinized for explosive decomposition was the ferroceno-fused dibenzo-dodecadehydro[18]annulene (**49**) (Scheme 7). Thermolysis of

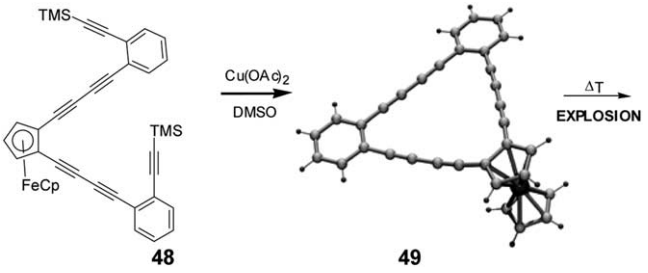

Scheme 7. Explosion of an organometallic dehydro[18]annulene. Note that the dehydroannulene structure is determined by single-crystal X-ray crystallography.

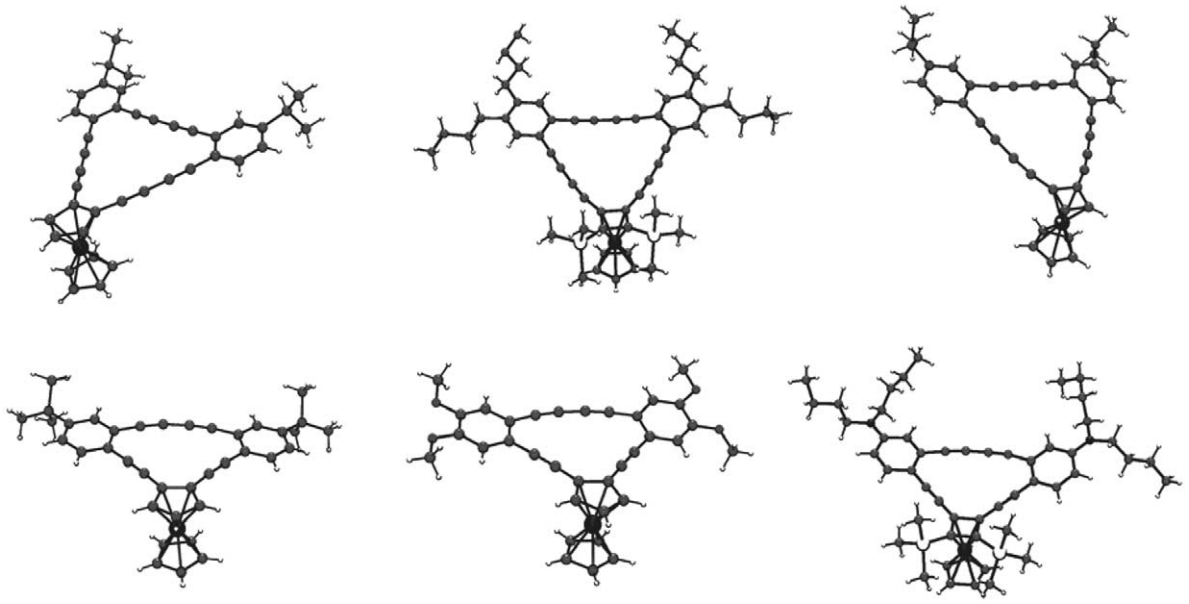

Fig. 5. Ball-and-stick representations of single crystal structure determinations of several organometallic dehydrobenzoannulenes.

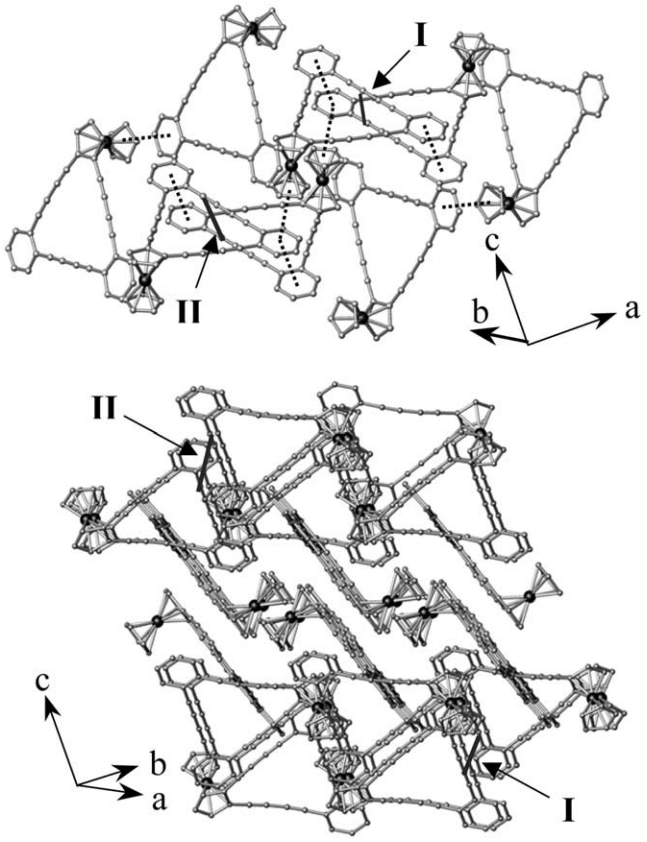

Fig. 6. Packing diagram of the exploding ferrocene cycle **49**. Disordered solvent molecules (dichloromethane and hexanes) are omitted. Crystallographic axes are included for orientation. Top: centroid–centroid (shown with dotted lines) and C_{alkyne}–C_{alkyne} distances (shown in red) are in the range of 3.59 (distance **I**) and 3.68 Å (distance **II**). The interplanar angles between neighboring phenyl rings are close to 7°. Bottom: Alternate view of the π–π stacks (horizontal and into the Figure).

microcrystalline powders of **49** did not give defined nanomaterials. If, however, single crystalline samples of **49** were heated, they exploded above 210 °C to furnish soot composed of defined carbon nanostructures. The nanomaterial formed in almost quantitative yields. In Fig. 6 the solid-state packing of **49** is shown; it is different from the packing of all of the other cycles that were analyzed by X-ray crystallography. There are numerous close contacts between the diyne units in **49** (see Fig. 6), that are in the range of the sum of the van der Waals radii (3.6 Å) of sp-carbons. Such interactions of the diyne groupings are observed in **49** but in none of the other organometallic dehydroannulenes. These contacts may be the key for its specific reactivity.

In Fig. 7 the bagel-shaped nanostructures resulting from pyrolysis of **49** are displayed. Upon examination at higher magnification, there is internal structure discernible that increases slightly upon prolonged annealing at 800 °C. What exactly these nanostructures are is hard to say; they could be either carbon toroids or large onion-shaped mega-fulleroids. Further examination of these bagels is ongoing.

The explosive thermal decomposition of the ferrocene-fused dodecadehydro[18]annulene (**49**) furnishes carbon nanomaterials with a rope- or onion-like internal structure. Currently, we are investigating the introduction of heteroatoms into organometallic dehydro[18]annulenes. It is likely that the presence of heteroatoms will affect the formation and structures of the explosion-generated carbon nanostructures.

5. Complex organometallic nanostructures based on cyclobutadiene(cyclopentadienyl)cobalt and ferrocene [78–81]

5.1. Butterfly-shaped organometallic topologies: from covalent synthesis to supramolecular ordering

This section highlights the synthesis and characterization of large butterfly-shaped, double dehydroannulenes

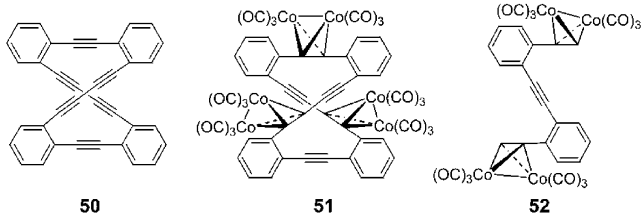

Scheme 8. Carbon rich compounds that form defined carbon nanostructures upon pyrolysis.

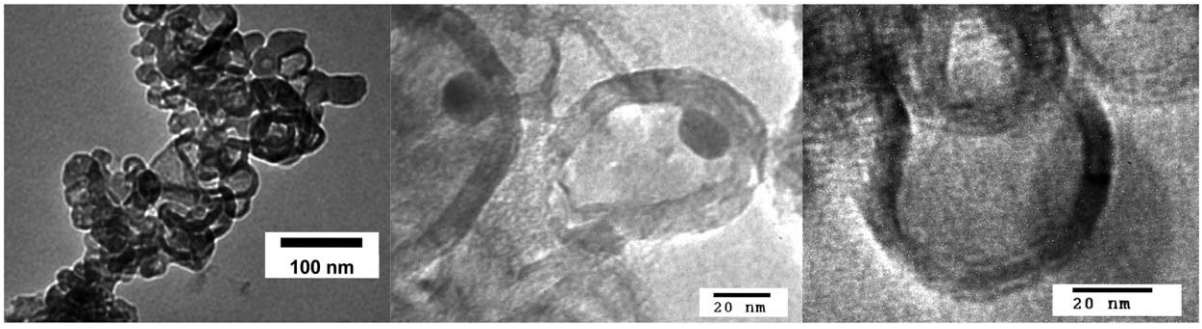

Fig. 7. Transmission electron micrographs of carbon nano-structures, formed by explosion of the organometallic dehydroannulene **49**.

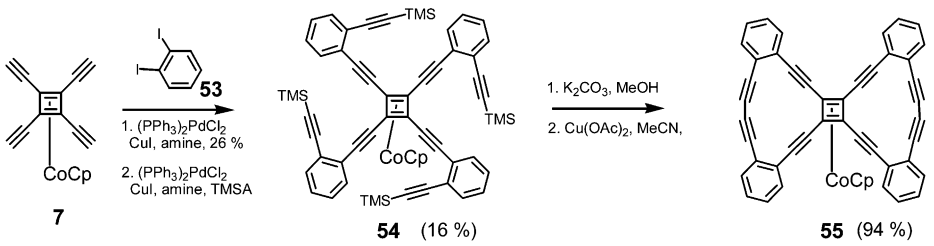

Scheme 9. Synthesis of the parent cyclobutadiene(cyclopentadienyl)cobalt hexadehydro[14]annulene-based butterfly.

that feature a central tetraethynylated cyclobutadiene complex. Such butterfly topologies are speculated to be important in the primary stages of the formation of fullerenes in the gas phase [72]. Pd-catalyzed coupling of **7** with *ortho*-diiodobenzene (**53**) and subsequent Pd-catalyzed coupling to trimethylsilylacetylene gives the polyyne **54** in an overall yield of 4.2% (Scheme 9). Desilylation of **54** is followed by ring closure utilizing the Vögtle variant [73] of the Eglinton coupling to form **55** in a 94% yield. The double ring closure is, therefore, an effective process.

The butterfly **55** is only sparsely soluble in organic solvents; a ^{13}C-NMR spectrum could be obtained in THF-d_8, however, it was not possible to grow a specimen useful for X-ray diffraction. To increase the solubility of the butterflies, and obtain derivatives that would crystallize better, a second, stepwise synthetic approach was developed. As shown in Scheme 10, **56** was transformed into the dehydroannulene **58** by standard Pd-methodology in a 50% overall yield. The intermediate **58** was deprotected and subjected to reactions 1–3. This sequence furnished the unsymmetrical bowtie **59** (57%) and the symmetrical bowtie **60** (16%). While the bowtie **59** is quite unstable, **60** is robust and readily soluble in hexanes, dichloromethane, and THF. Crystallization from dichloromethane furnished suitable single crystals (vide infra). To obtain butterflies that incorporate dehydro[18]annulenes, a similar stepwise approach was utilized. A dehydroannulene moiety was attached to **61** by coupling the brominated 1,2-diethynylbenzene derivative **62** to **61** (Scheme 11) [74,75]. Subsequent deprotection was followed by Vögtle ring closure to afford **63a** with isopropyl (28%) or **63b** (R = butyl, 38%) substituents. Deketalization of **63** by *para*-toluenesulfonic acid (TsOH) is facile and the intermediate aldehydes were subjected to an Ohira–Taber–Bestmann alkynylation. The tetraethynylcyclobutadiene cycles **64** were obtained in 17% (R = isopropyl) and 18% (R = butyl) overall yield; they are unstable when isolated.

The cyclic intermediates **64** allowed the attachment of the second dehydroannulene moiety as shown in Scheme 11. Deprotection and ring closure with $Cu(OAc)_2$ in acetonitrile furnishes **66** in moderate yields. For the synthesis of the mixed bowtie **67**, **64b** (R = butyl), is coupled to **65**; the TMS-groups are cleaved by K_2CO_3. The second ring is closed by $Cu(OAc)_2$ to furnish **67** in an overall yield of 51%. Attempts to grow specimens of **66a** or **66b** failed, but it was possible to obtain suitable single crystals of **67** from dichloromethane/hexane mixtures. All butterflies **60**, **66**, and **67** are stable as solids under ambient conditions.

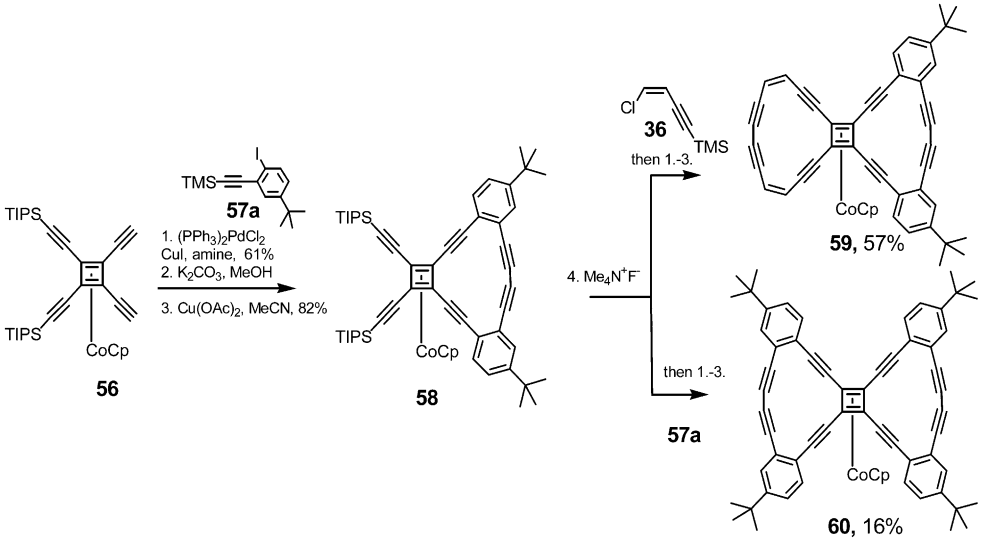

Scheme 10. Synthesis of the *tert*-butyl-substituted, hexadehydro[14]annulene-based butterflies.

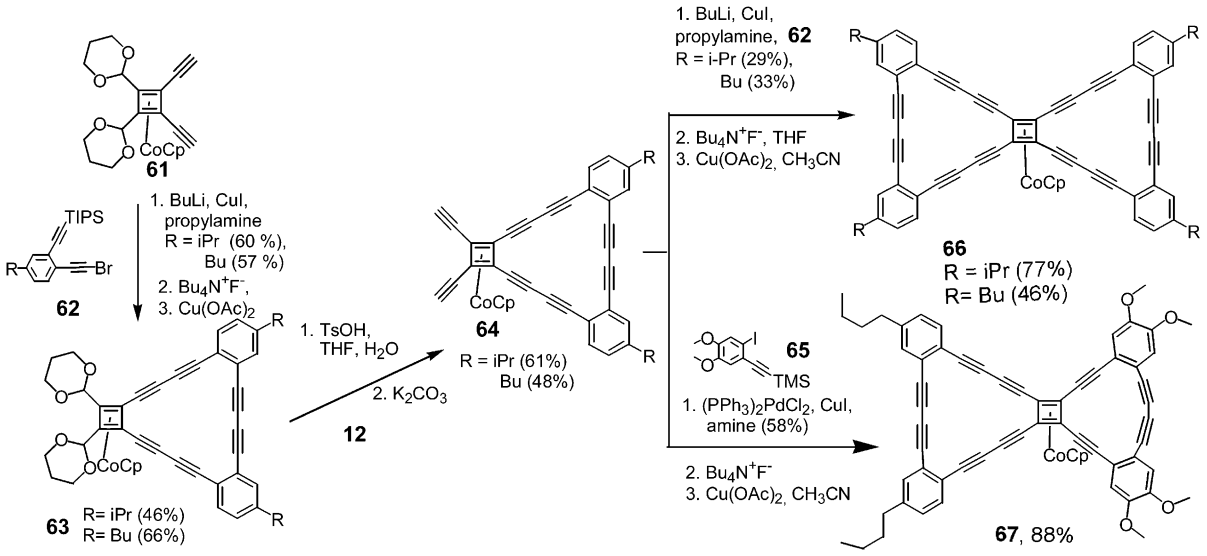

Scheme 11. Synthesis of large butterflies.

5.1.1. Single crystal structures of the butterflies

To gain a better understanding of structure, topology and supramolecular ordering of the butterfly **60** in the solid state a suitable single crystal was subjected to X-ray diffraction. Fig. 8a displays the ORTEP representation of **60**. The significant upward bend in the large hydrocarbon ligand is of electronic origin and not a packing effect according to semiempirical quantum chemical calculations (PM3 TM, Spartan). The solid state ordering of **60** is spectacular, featuring a tetragonal

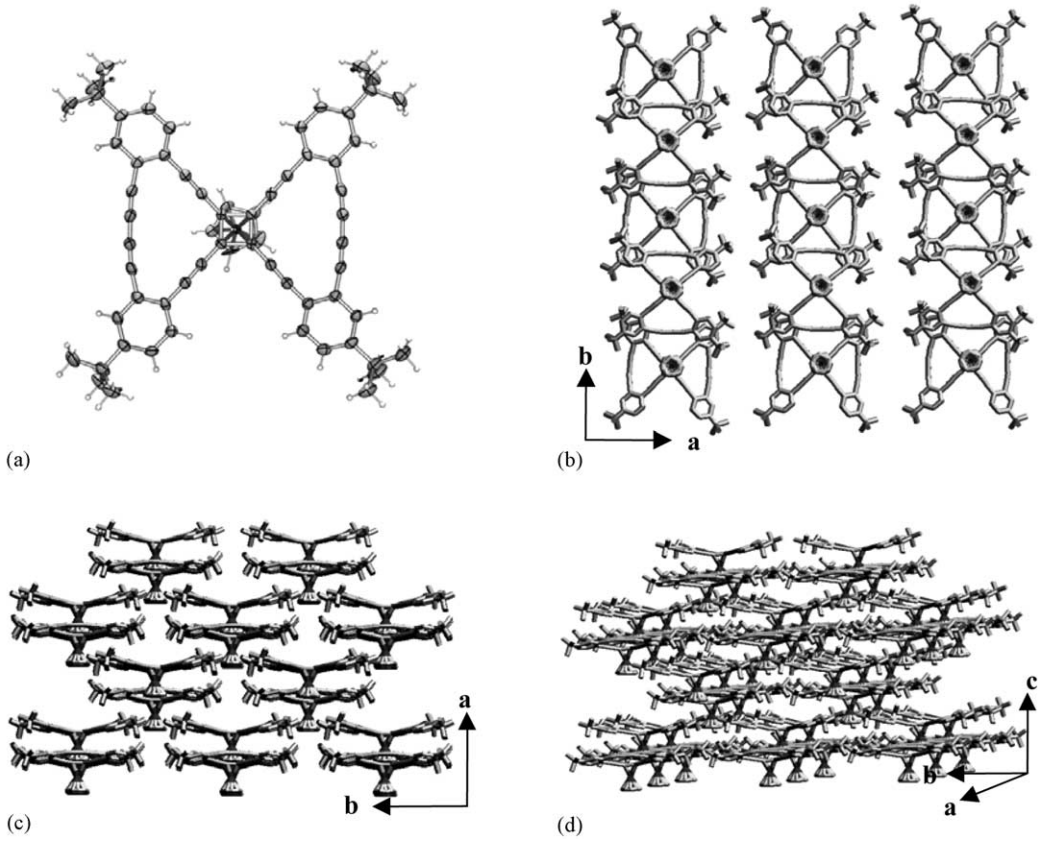

Fig. 8. (a) ORTEP representation of the small butterfly **60**. (b–d) Packing of the organometallic butterfly **60**. The packing pattern is such that the hydrocarbon ligands in two adjacent layers are packed in a staggered fashion. The molecules in each layer are rotated by 90° with respect to each other, which gives an overall tetragonal symmetry to this packing arrangement.

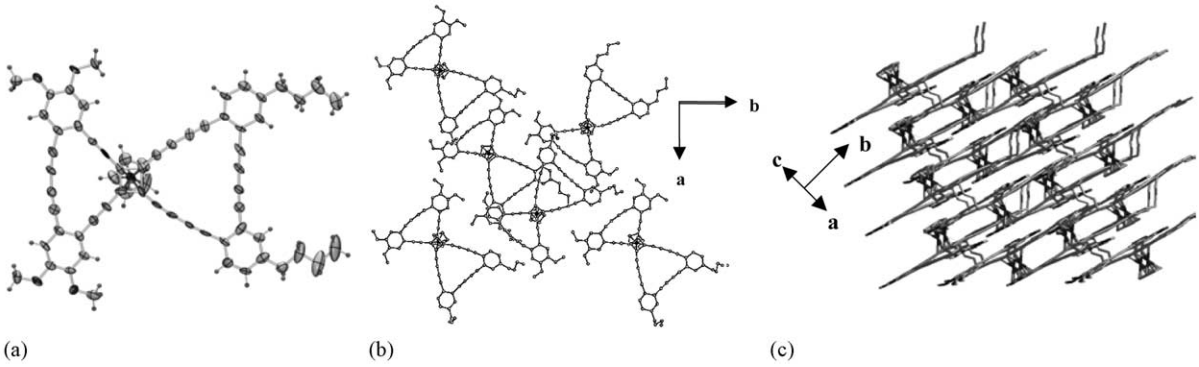

Fig. 9. (a) ORTEP representation and packing of the unsymmetrical butterfly **67** in the solid-state. (b) View onto the large hydrocarbon ligand. (c) Layered structure of **67**. The layers are spaced ca. 3.6 Å spaced apart, with the CpCo units and the butyl groups filling the interstitial interlayer spaces.

packing of the molecules in the space group $I4_1$, quite unusual for an organometallic compound. Fig. 8b–d shows views of the packing of **60**. The molecules are stacked in an AB scheme along the vertical *c*-axis. In two different layers the molecules are rotated by 90° with respect to each other. In a single plane (Fig. 8) the molecules are arranged as chessboard tiles in which every second row of 'tiling' is missing.

The second layer above or below fills the 'empty' spaces above and below the squares in the middle. The net effect is a striking supramolecular arrangement of **60**. The organometallic cyclobutadiene(cyclopentadienyl)cobalt units are arranged in a square grid-like pattern that repeats the tetragonal symmetry of the cyclobutadiene complex.

In Fig. 9a the ORTEP representation of the unsymmetrical butterfly **67** is shown. The molecular structure is the expected combination of a dehydro[14]annulene and a dehydro[18]annulene. The bond lengths and bond angles are in excellent agreement with published values for the corresponding sub-structures [26,45–48]. While **60** is significantly bent, the large hydrocarbon ligand of **67** is planar. Calculation of **67**'s structure by PM3 TM shows that the hydrocarbon ligand is even more bent (21.4° for the dehydro[18]annulene and 17.5° for the dehydro[14]annulene) than the one in **60**. The observed planarity in the solid-state arrangement of **67** must be due to a packing effect: The ordering of **67** in the solid state is somewhat similar to that of **60**, the molecules are packed on top of each other and rotated by 90°. In Table 1 the cell parameters of **60** and **67** are listed; while the *a* and the *b*-axes of **60** and **67** are different, their *c*-axes are similar. The *c*-axis is the 'layer' axis along which the molecules are stacked on top of each other. The slightly larger *c*-axis of **60** is due to its larger *tert*-butyl substituents and the upward bending of the whole hydrocarbon ligand. Both factors contribute to the increased 'thickness' of **60** compared to **67** that must

Table 1
Crystallographic data for **60** and **67**

	60	**67**
Crystal system	Tetragonal	Monoclinic
Space group	I4(1)	Cc
Unit cell dimensions		
a (Å)	19.156(5)	32.447(3)
b (Å)	19.156(5)	27.437(3)
c (Å)	15.842(7)	14.042(1)
α (°)	90	90
β (°)	90	108.354(2)
γ (°)	90	90
V (Å^3)	5814(3)	11865 (2)
Z	4	8

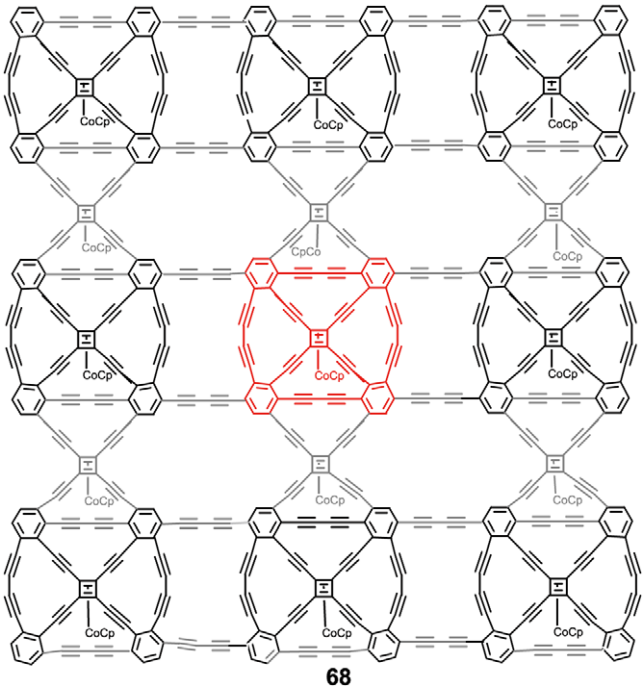

Fig. 10. Hypothetical covalent network version **68** of the supramolecular assembly formed by the butterfly **60**. The herein synthesized modules are colored black, while the connectors are colored grey. The red center represents an organometallic wheel.

be accommodated by the crystal lattice. In both **67** and in **60**, the large hydrocarbon ligands, located in a common plane, are rotated by 90° with respect to each other. The butyl 'tails' of **67** are tucked in-between two layers, the interstitial space. The main differences in the fascinating packing and in the unit cells arise therefore from the differing dimensions and shapes of the large π-conjugated ligands in **60** and in **67**.

A family of novel butterfly-shaped organometallic double dehydro[14]annulenes and dehydro[18]annulenes has been prepared by a combination of Pd- and Cu-catalyzed reactions. These are attractive synthetic targets on the way to an all-butadiyne bridged organometallic wheel (see red sub-structure in Fig. 10). The most surprising feature of the organometallic butterfly **60** is its supramolecular ordering in the solid state, the formation of an unusual tetragonal network. Importantly, according to Jarrold and coworkers [72] all-carbon topologies of the butterfly-type described here could play an important role in the first stages of fullerene formation in the gas phase. In future the pyrolysis of the organometallic butterflies will be carried out to see if defined carbon nanostructures will form.

5.2. *Higher cross-connected organometallic topologies: synthesis of organometallic half-wheels and an organometallic seco-wheel [80,81]*

The successful completion of the synthesis of the butterfly-shaped organometallic nano-objects let us explore the construction of other organometallic carbon-rich topologies. In this section the synthesis of a seco-wheel (seco, latin: cut open) and an organometallic half-wheel are discussed. The synthetic strategy employed is a mix-and-match approach utilizing building blocks that were already at hand. The synthesis of **74** (Scheme 12) commences with the coupling of **69** to a protected 3,5-diethynyl-4-iodo-butylbenzene (**70**). The coupling is not very efficient (23%) as a consequence of the structure of the aromatic iodide. In the second step

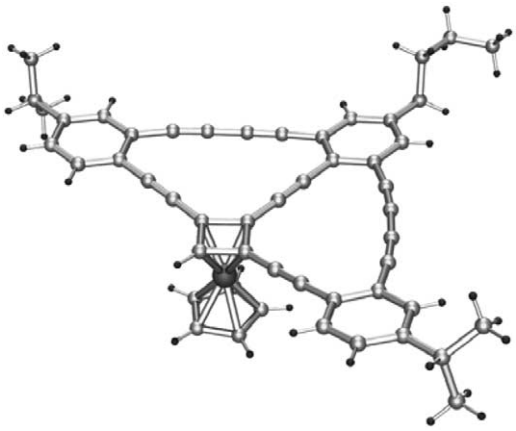

Fig. 11. Ball-and-stick plot of the cyclobutadiene(cyclopentadienyl)cobalt-based organometallic half wheel **74**.

the ketal groups of **71** are stripped off and the resulting dialdehyde is transformed into the diyne **72**. Pd-catalyzed coupling of **72** to the iodide **57b** occurs cleanly to give **73** (70%). The silyl protecting groups are removed by $Bu_4N^+F^-$ and double cyclization of the terminal alkynes by $Cu(OAc)_2$ furnishes the half-wheel **74** in 71% yield as yellow crystalline material. Single crystals of **74** were obtained from dichloromethane–hexane mixtures. The molecular structure of **74** is shown in Fig. 11. Bond lengths and bond angles are in excellent agreement with published values for cyclobutadiene complexes and benzodehydroannulenes. The structure is largely unstrained due to the fit of the involved bond angles in this topology. The bending in the diacetylene bridges is only moderate and does not appear to decrease the yield of the ring closure.

The half-wheel concept was expanded to the ferrocene nucleus (Scheme 13). The successful synthesis of pentaethynylferrocene delivered mixed acetal/alkynyl substituted ferrocenes. Starting from ketal **75**, double coupling to **57b** gave **76**. Deketalization of **76** by TsOH and conversion of the intermediate aldehyde into a **77** was followed by coupling to **70** leading to

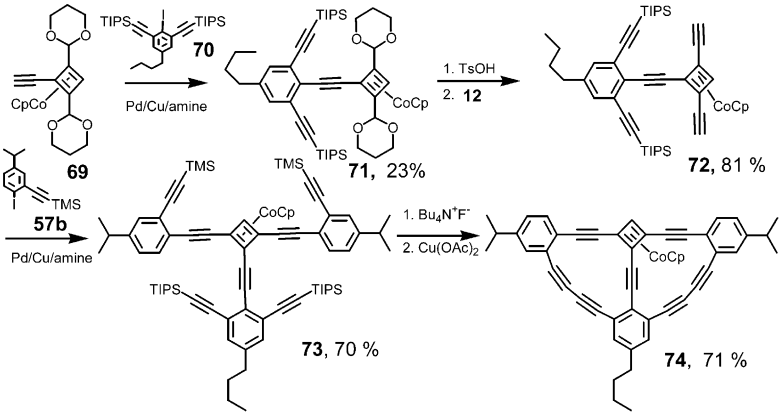

Scheme 12. Synthesis of an organometallic half wheel **74**.

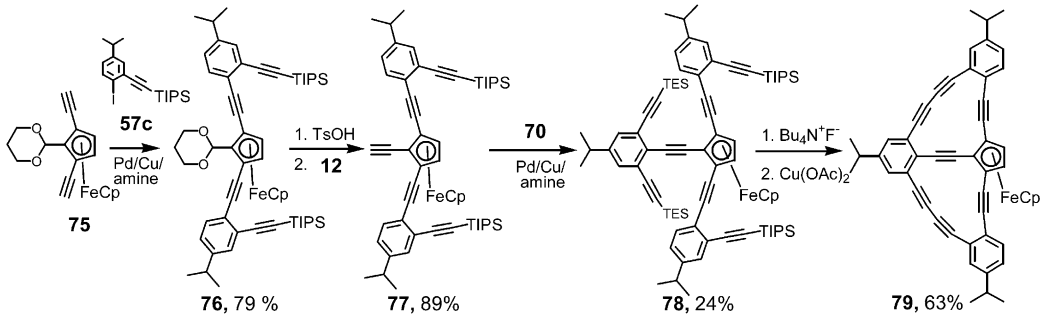

Scheme 13. Synthesis of an organometallic half wheel **79**.

the silylated intermediate **78**. After deprotection copper-mediated cyclization of **78** yields the ferrocene-based half wheel **79** in 63% yield. It was not possible to obtain a mass spectrum of **79**, but single crystals were obtained from a mixture of hexanes and dichloromethane. Fig. 12 shows a ball-and-stick representation of the molecular structure of **79**. The gross features are similar to those found in the smaller cyclobutadiene analog **74**, however, the two outer alkyne spokes that connect the ferrocene nucleus to the benzene units are somewhat bent to counteract the slight misfit of the bond angles. In Fig. 12b the packing of **79** is shown. The molecules form a 6/1 triple helix in the crystalline lattice featuring a rhomboid symmetry. The ferrocene half wheel displays an interesting nano-tubular arrangement in the solid state.

To access the seco-wheel structure **83** that is derived from the small butterfly **60**, one would formally have to insert a butadiyne bridge between two of the unconnected benzene rings: The synthesis of **83** starts with the Pd-catalyzed coupling of **57d** to **62** (Scheme 14) that furnishes **80** in 59% yield.

Deketalization of **80** is followed by Ohira alkynylation to give the intermediate **81**. The subsequent coupling of **81** to **70** is difficult and furnishes the protected intermediate in only 16% yield. Full deprotection of the silyl groups by tetrabutylammonium fluoride is followed by Vögtle cyclization of **82** to supply the triply closed seco-wheel **83** (25%). The efficiency per ring closure is 63%. While the yield of the triple ring closure is not high, one has to consider that part of the starting material **82** is consumed (Scheme 15) in a non-productive cyclization. Heavily crosslinked insoluble materials form via intermediates such as **84**.

The spectacular molecular structure of **83** mandated the growth of a specimen for single crystal X-ray diffraction. Fig. 13 shows the ORTEP representation as final proof of the topology of **83**. The contiguous connection of three of the benzene rings by diyne units has considerably flattened out the large hydrocarbon ligand. A semiempirical calculation (PM3 TM) shows that the 'flattening' is not a crystal packing effect but seems to be an innate property of the molecular geometry. According to PM3 TM the introduction of the fourth diyne bridge would lead to a planar π-system.

The synthesis of the closed wheel (Scheme 16) was attempted, but coupling four of the tetrasubstituted iodobenzens **70** to the cyclobutadiene core failed. The direct coupling of **70** to the tetraethynylcyclobutadiene **7** did not give isolable material, only dark decomposition

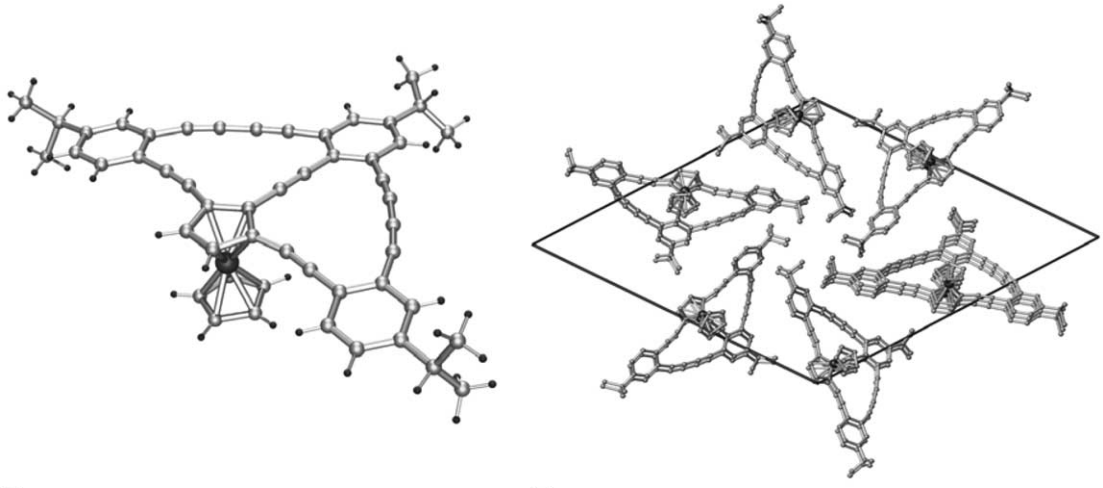

Fig. 12. Single-crystal XRD of **79**. (a) Ball-and-stick plot of the molecular topology. (b) Packing of **79** in the solid state.

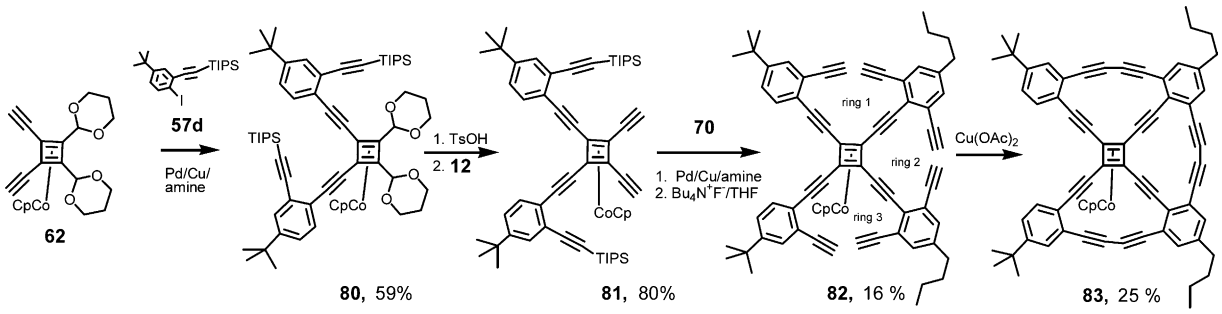

Scheme 14. Synthesis of an organometallic seco-wheel **83**.

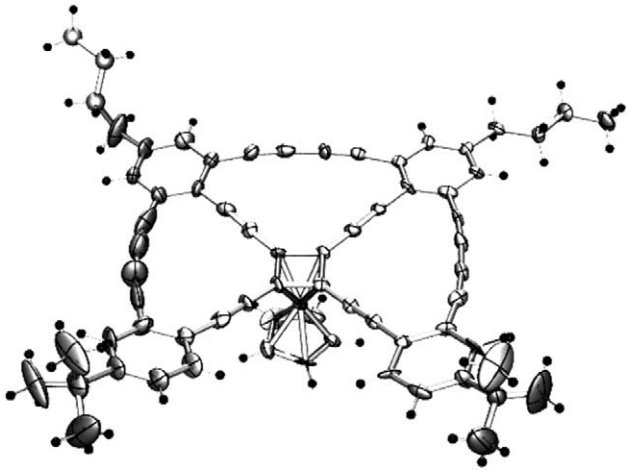

Fig. 13. ORTEP representation of the seco-wheel **83**. The large hydrocarbon ligand is flattened out and much less bent than the hydrocarbon ligand in the butterflies (see Fig. 8).

products. In the stepwise approach (see Scheme 16) the first coupling of **70** to the core **62** worked to give **85**, albeit in only 12% yield. The subsequent deketalization–alkynylation sequence was hampered by the steric bulk of the TIPS-groups that allowed the isolation of the intermediate **86** in only 22%. Starting material was recovered. Attempts to couple the minute amounts of **86** to **70** now failed under different conditions because of the combined steric hindrance at both the iodide and the diyne unit. We concluded that the synthesis of the intermediate **87** will be difficult at best or impossible. Consecutive low yields in this multistep process are a crippling blow to the synthesis of the desired wheel.

6. Organometallic dendrimers [82]

An extension of the herein showcased chemistries was the quest for larger tetraalkynylated cyclobutadiene(cyclopentadienyl)cobalt complexes such as **89**. In this complex, the alkynes are removed from the cyclobutadiene unit by an intermittent benzene ring. $CpCo(CO)_2$-mediated reaction of the bis-TIPS-protected diethynyltolane derivative **88** (Scheme 17) furnished **89** in 62% yield after deprotection with tetrabutylammonium fluoride. The tetrayne **89** is stable. A single-crystal X-ray structure of **89** could be obtained. It shows a paddle-shaped conformation of the phenyl rings similar to that observed in tetraphenylcyclobutadiene(cyclopentadienyl)cobalt (Scheme 17). The availability and stability of **89** made it a suitable precursor for the synthesis of organometallic dendrimers of the Müllen-type [83,84]. Reaction of **89** and tetraphenylcyclopentadienone furnished the dendrimer **90**. The concept was extended by utilizing cyclobutadiene complexes **91** and **93** to give the *meta*-dendrimer **92** and the double *meta*-dendrimer **94** (Scheme 18). The dendrimers formed in high yield, are stable compounds and were fully characterized. It was of interest to compare the physical properties of the three dendrimers with respect to their relative size. Two of the dendrimers, **90** and **92**, are isomers, while the third one, **94**, is larger.

Attempts to grow single crystals **90**, **92** or **94** failed. As a consequence (Fig. 14) semiempirical calculations were performed utilizing the PM3 (TM) basis set for the molecular structure evaluation of the dendrimers. The *para*-dendrimer **90** has a defined, rigid, and extended molecular conformation (left) that (probably) represents

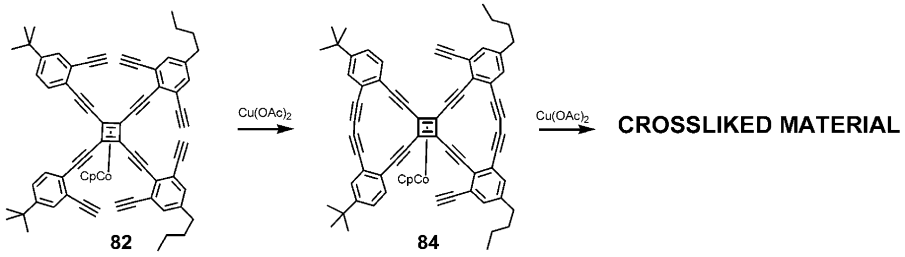

Scheme 15. Undesired crosslinking of the seco-wheel precursor.

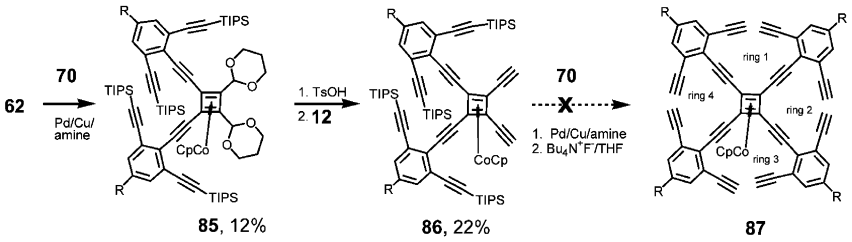

Scheme 16. Attempted synthesis of the all-closed organometallic wheel.

the global energy minimum. In the cases of **92** and **94** (middle, right) representative conformations that are local minima are shown. The global structural minima of these complexes would have to be calculated by molecular dynamics methods. The floppy *meta*-dendrimer (**92**, middle) is significantly less voluminous than its *para*-isomer **90**. To demonstrate this effect quantitatively we performed high-resolution gel permeation chromatograpy (HGPC, see Fig. 15) on **90**, **92** and **94**. In HGPC the hydrodynamic volume (i.e. size) is inversely correlated with the elution time. Thus, the large dendrimer **94** (Fig. 15) elutes first, followed by the extended dendrimer **90**, while the compact *meta*-isomer **92** elutes last. This experiment demonstrates that the size of isomeric dendrimers can vary significantly. The electrochemistry of the three dendrimers was examined, but the change in the oxidation potential when going from tetraphenylcyclobutadiene(cyclopentadienyl)cobalt to the open **90** to the compact dendrimer **94** was small, suggesting that electron transfer in these materials is not particularly dependant upon the presence or absence of an 'isolating' hydrocarbon shell.

7. Organometallic polymers [85–87]

The creation of nanostructures and self-assembled materials makes the synthesis, structural elucidation and study of self-assembly of organometallic poly(aryleneethynylene)s (PAE **97**, **99**) with cyclobutadiene units in the main chain an attractive proposition. Earlier a PAE similar to **97** was reported in which the benzene rings were hexyl substituted (Scheme 19) [87]. The PAE **97** is thermotropic liquid crystalline, forming a nematic phase, it is the first thermotropic conjugated organometallic polymer. Utilizing different diiododialkylbenzene co-monomers (**96**) extends the concept. Variation of the side chains should control supramolecular behavior and result in novel self-assembled materials **97**. An increase of the ratio of benzene to cyclobutadiene rings would establish a second handle to change the supramolecular properties of the formed polymers.

Alkyne metathesis of a dipropynylated monomer **98** (Scheme 20) furnished **99** in almost quantitative yields as high molecular weight, yellow-to-tan materials featuring a variety of side chains on the benzene rings. In both series, **97** and **99** chiral polymers were available by attachment of chiral 3,8-dimethyloctyl side chains to the benzene rings in the monomers.

7.1. Optical and chiroptical properties

The synthesis of the organometallic polymers **97** and **99** allowed the investigation of their optical properties. A representative series of UV–vis spectra of **97** in solution, in a poor solvent, and as thin film is displayed in Fig. 16. Conjugated polymers often show a distinct aggregation behavior in which the UV–vis bands are

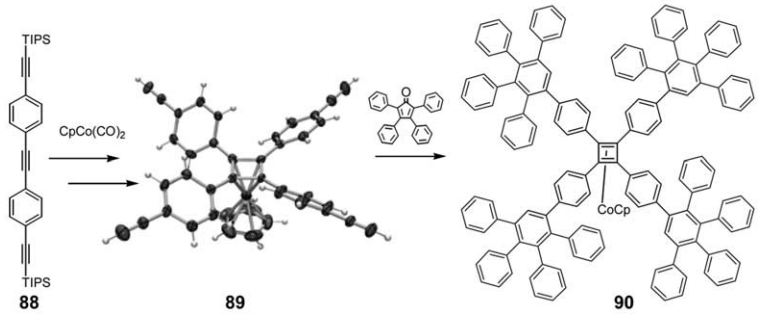

Scheme 17. Organometallic dendrimers utilizing a tetraphenylcyclobutadiene core.

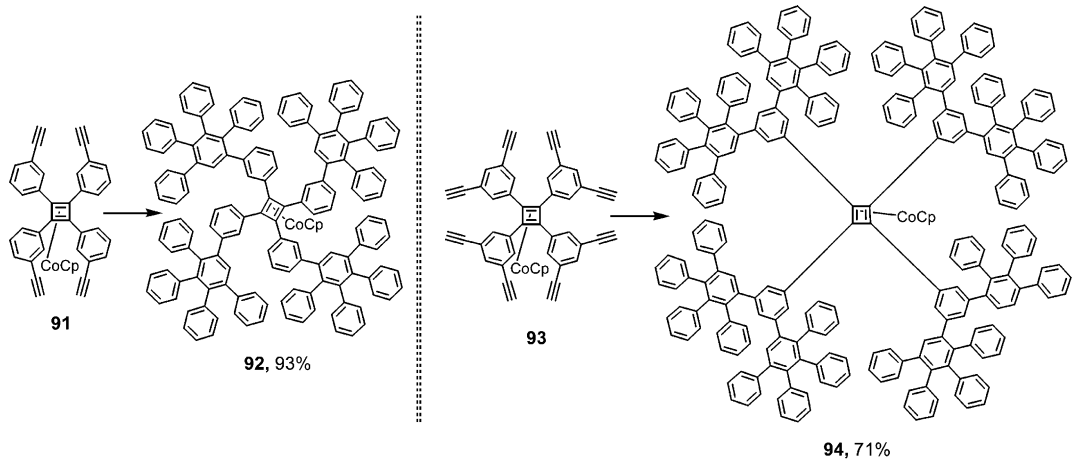

Scheme 18. Synthesis of organometallic dendrimers utilizing a tetraphenylcyclobutadiene core.

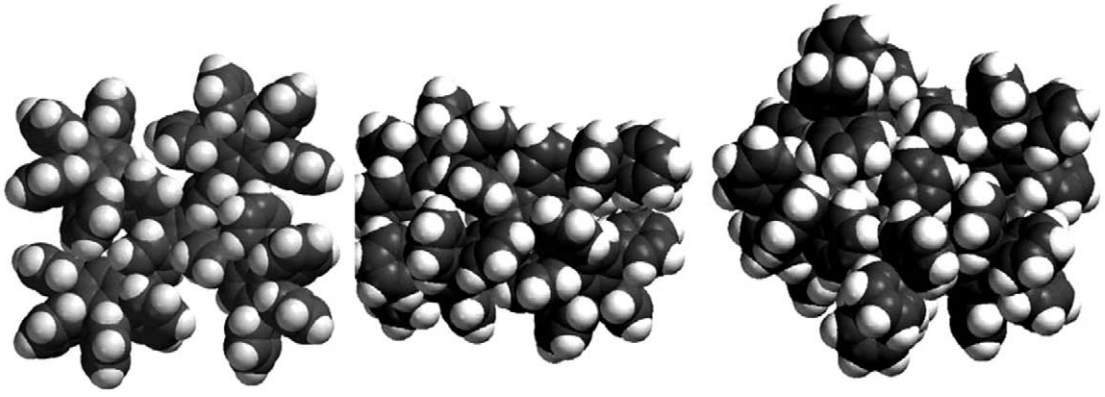

Fig. 14. PM3-TM optimized structures of organometallic dendrimers. *Para* (left, **90**), *meta* (middle, **92**), *meta-meta* (right, **94**).

significantly shifted upon addition of a non-solvent or upon going into the solid state, i.e. thin films [88–91]. Not so the polymers **97** and **99**. Their solution, aggregation, and thin film UV–vis spectra are almost superimposable and did not show significant shifts. To explore this behavior further, the circular dichroism (CD) of the chirally substituted polymer **97** was investigated. Chiroptical activity was absent in the chiral copolymer **97** both in solution and in thin films. The result is surprising in the light of the fact that 'regular' PPEs [90] show very large chiroptical activities as a result of supramolecular ordering into nanoscopic fibrils.

The chirally substituted copolymer **99** (made by alkyne metathesis) was investigated too, and a bisignate ($g = 2(\varepsilon_R - \varepsilon_L)/(\varepsilon_R + \varepsilon_L) = -0.0059$; Fig. 17) but small chiroptical signal was detected upon addition of methanol (non solvent) to a solution of **99** in chloroform. According to Meijer and coworkers [91] a bisignate chiroptical response is a strong indication for an interchain electronic interaction. This phenomenon is a consequence of to the Davidov split of interacting chromophores [92,93].

The polymer chains in **99** show a small but measurable interchain interaction, but it is not clear if and how

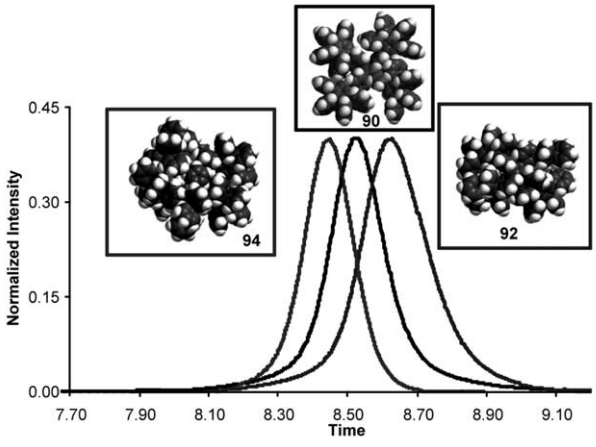

Fig. 15. Gel permeation chromatograms of the organometallic dendrimers **90**, **92** and **94**.

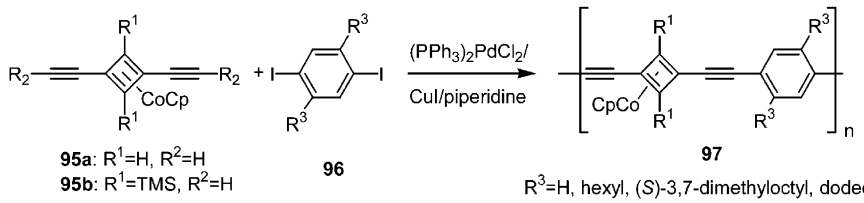

Scheme 19. Synthesis of cyclobutadiene(cyclopentadienyl)cobalt containing poly(aryleneethynylene)s by Pd-catalyzed coupling methods.

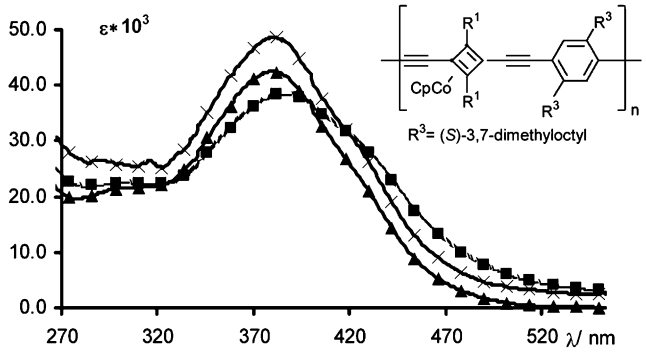

Fig. 16. UV–vis spectrum of an organometallic polymer **97** in solution ($CHCl_3$, – × –), in the aggregated state (CH_3OH/–$CHCl_3$, –■–), and in thin films (–▲–).

much the conformation of single chains play a role. To get a qualitative understanding a PM3 TM calculation was performed on a model octamer **100** (Fig. 18). The bulky TMS groups and CpCo-units lead to a situation where the backbone of **100** is protected from interacting with other polymer chains. The absence of a chiroptical effect is thus due to steric hindrance that does not permit interchain interactions. The chiral side chains are probably tucked into the interstitial space and do not seem to induce chiral order into the solid state packing of **97**. Consequently this packing arrangement negates the influence of the chiral dimethyloctyl side chains on the conformation of the polymer backbone, which is different from the case of the chirally substituted PPEs that show large chiroptical responses in thin films [90]. The polymer **99** represents an intermediate case where some interchain interactions are possible despite the presence of the bulky cyclobutadiene(cyclopentadienyl)cobalt units.

7.2. Self assembly in thin films: transmission electron microscopy (TEM) and polarizing microscopy

To finish the investigation of the organometallic polymers, polarizing and electron microscopies were performed on thin film samples. The polymers **97** are highly ordered and form nicely lamellar structures (Fig. 19). Despite the lack of direct intermolecular interactions of the π-backbones of **97**, which would have been detected by UV–vis and CD spectroscopies, it is highly organized in the solid state (Fig. 19). An important aspect of this behavior is the orientation of the polymer chains with respect to the nanoscale features. In regular PPEs, the polymer chains are aligned along the long axis of the lamellar structures [61,85]. In the organometallic polymers **97** the chains of the macromolecules are aligned perpendicularly to the long axis of the lamellae. The width of the lamellae found in the organometallic PAEs **97** coincides with length of an extended polymer chain obtained by multiplying the degree of polymerization (P_n) with the length of a repeating unit. One repeating unit is 1.1 nm, the P_n obtained by gel permeation chromatography (GPC) was 25, and thus the length of an extended polymer chain of **97** is 28 nm. The lamellar features seen in Fig. 19 are approximately 30 nm thick and correspond well to the length of single extended macromolecules. Polymers with increasing P_n have wider lamellae; the relation of width of lamella versus P_n held for all samples that were examined. These

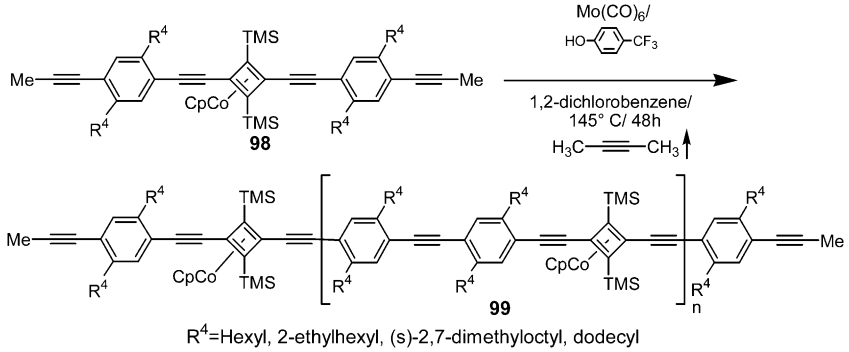

Scheme 20. Synthesis of a cyclobutadiene(cyclopentadienyl)cobalt containing poly(aryleneethynylene) by the ADIMET route.

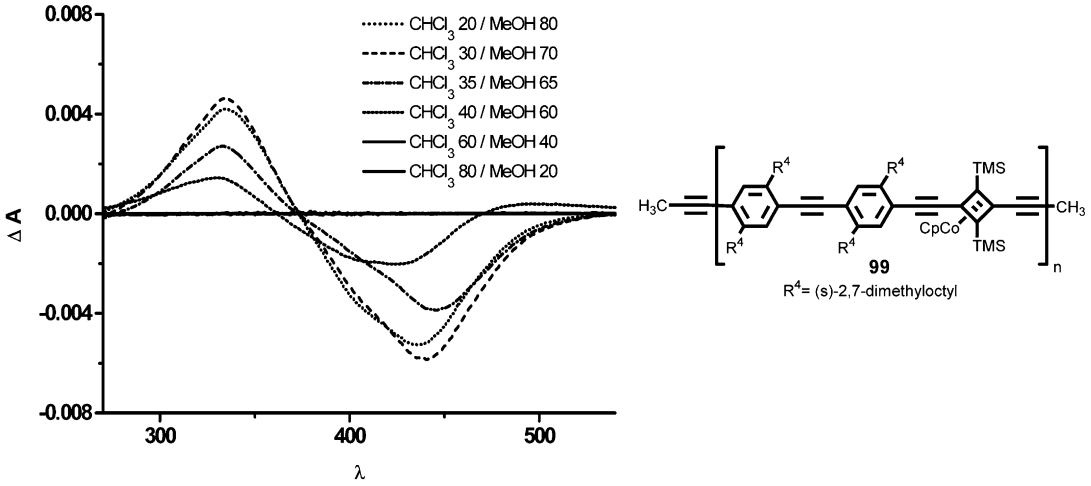

Fig. 17. CD spectrum of an organometallic copolymer **99** in solution and upon addition of the non solvent methanol. Maximum CD signal is recorded in an 80/20 solution of methanol/ chloroform with $g = -0.0059$.

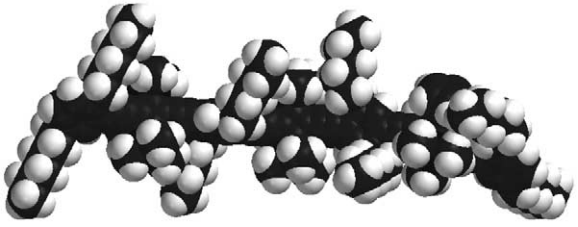

Fig. 18. Single chain conformation of an organometallic tetramer 100.

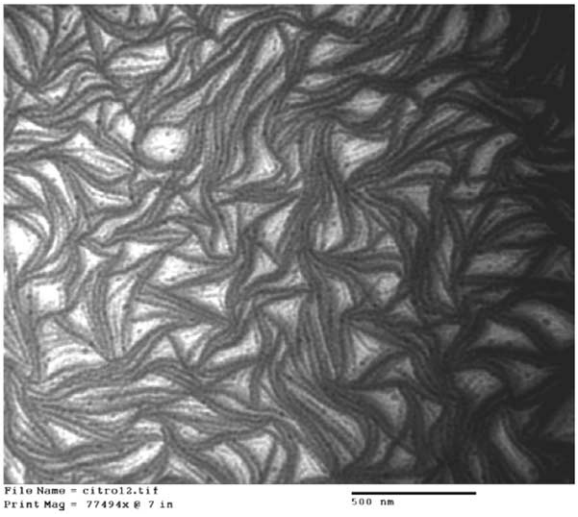

Fig. 19. Electron micrograph of a highly lamellar phase of **97**. The width of the strands corresponds to the backbone length of the polymers.

data and supporting electron diffraction studies confirm the difference in the packing of PPEs and organometallic PAEs **97**. The differences in the packing pattern must be responsible for the greatly differing optical and chiroptical properties of PPEs and the organometallic PAEs **97** and **99**.

8. Conclusions

Multi-alkynylated cyclobutadiene(cyclopentadienyl)cobalt complexes and ferrocenes are versatile building blocks for the construction of organometallic dehydroannulenes, carbon-rich scaffolds, novel bagel-shaped carbon nanostructures, and monomers for conjugated organometallic polymers. The highly alkynylated sandwiches show a chemistry that shares some communalities with their simpler benzene analogs but dramatically extends and varies this fascinating subject and makes alkynylated π-complexes a fruitful research area.

Acknowledgements

We thank the National Science Foundation (PI Bunz, CAREER, CHE 9981765), the Petroleum Research Fund (1998–2000), the Deutsche Forschungsgemeinschaft (1994–1997), the Stiftung Volkswagen (1993–1997), and the USC NanoCenter for generous funding. UB is a Camille Dreyfus Teacher-Scholar (2000–2004). We thank Dr. M.D. Smith (USC) for his invaluable help determining the single crystal X-ray structures of most of the herein mentioned compounds.

References

[1] M. S. Dresselhaus, G. Dresselhaus, P. C. Eklund, Science of Fullerenes and Carbon Nanotubes, Academic Press, San Diego, 1996.
[2] L.T. Scott, M.M. Boorum, B.J. McMahon, S. Hagen, J. Mack, J. Blank, H. Wegner, A. de Meijere, Science 295 (2002) 1500.
[3] For carbon nanotube formation see: M. Terrones, W.K. Hsu, H.W. Kroto, D.R.M. Walton, Top. Curr. Chem. 199 (1999) 189.
[4] S. Iijima, Nature 354 (1991) 56.

[5] (a) P.M. Ajayan, Chem. Rev. 99 (1999) 1787;
(b) D. Ugarte, Carbon 33 (1995) 989.
[6] (a) D. Ugarte, Carbon 32 (1994) 1245;
(b) W. For novel fullerenes containing four membered rings see, S.-C. Qian, R.B. Chuang, T. Amador, M. Jarrosson, S. Sander, S.I. Pieniazek, Y.R.ubin Khan, J. Am. Chem. Soc. 125 (2003) 2066.
[7] F. Diederich, Nature 369 (1994) 199.
[8] F. Diederich, Liebigs Ann.-Receuil (1997) 649.
[9] P. Siemsen, R.C. Livingston, F. Diederich, Angew. Chem. Int. Ed. Engl. 39 (2000) 2632.
[10] P. Manini, W. Amrein, V. Gramlich, F. Diederich, Angew. Chem. Int. Ed. Engl. 41 (2002) 4339.
[11] N.N.P. Moonen, C. Boudon, J.P. Gisselbrecht, P. Seiler, M. Gross, F. Diederich, Angew. Chem. Int. Ed. Engl. 41 (2002) 3044.
[12] J. Stahl, J.C. Bohling, E.B. Bauer, T.B. Peters, W. Mohr, J.M. Martin-Alvarez, F. Hampel, J.A. Gladysz, Angew. Chem. Int. Ed. Engl. 41 (2002) 1871.
[13] R. Dembinski, T. Bartik, B. Bartik, M. Jaeger, J.A. Gladysz, J. Am. Chem. Soc. 122 (2000) 810.
[14] R.D. Adams, B. Qu, Organometallics 19 (2000) 2411.
[15] R.D. Adams, O.S. Kwon, B. Qu, M.D. Smith, Organometallics 20 (2001) 5225.
[16] R.D. Adams, B. Qu, M.D. Smith, Inorg. Chem. 40 (2001) 2932.
[17] T.J.J. Müller, H.J. Lindner, Chem. Ber. 129 (1996) 607.
[18] S.H. Liu, Y.H. Chen, K.L. Wan, T.B. Wen, Z.Y. Zhou, M.F. Lo, I.D. Williams, G.C. Jia, Organometallics 21 (2002) 4984.
[19] H.P. Xia, W.F. Wu, W.S. Ng, I.D. Williams, G.C. Jia, Organometallics 16 (1997) 2940.
[20] K. Schlögl, H. Egger, Monatsh. Chem. 94 (1963) 376.
[21] K. Schlögl, W. Steyrer, Monatsh. Chem. 96 (1965) 1520.
[22] K.H.H. Fabian, H.J. Lindner, N. Nimmerfroh, K. Hafner, Angew. Chem. Int. Ed. Engl. 40 (2001) 3402.
[23] J.K. Pudelski, M.R. Callstrom, Organometallics 13 (1994) 3095.
[24] V.W.W. Yam, V.C.Y. Lau, K.K. Cheung, Organometallics 15 (1996) 1740.
[25] V.W.W. Yam, K.K.W. Lo, K.M.C. Wong, J. Organomet. Chem. 578 (1999) 3.
[26] U.H.F. Bunz, Y. Rubin, Y. Tobe, Chem. Soc. Rev. 28 (1999) 107.
[27] J.J. Pak, T.J.R. Weakley, M.M. Haley, J. Am. Chem. Soc. 121 (1999) 8182.
[28] M.M. Haley, J.J. Pak, S.C. Brand, Top. Curr. Chem. 121 (1999) 81.
[29] M.M. Haley, M.L. Bell, J.J. English, C.A. Johnson, T.J.R. Weakley, J. Am. Chem. Soc. 119 (1997) 2956.
[30] J.J. Pak, T.J.R. Weakley, M.M. Haley, Am. Chem. Soc. 121 (1999) 8182.
[31] R. Boese, A.J. Matzger, K.P.C. Vollhardt, J. Am Chem. Soc. 119 (1997) 2052.
[32] P.I. Dosa, C. Erben, V.S. Iyer, K.P.C. Vollhardt, I.M. Wasser, J. Am Chem. Soc. 121 (1999) 10430.
[33] R. Faust, Angew. Chem. Int. Ed. Engl. 37 (1998) 2825.
[34] L.T. Scott, in: P.J. Stang, F. Diederich (Eds.), Modern Acetylene Chemistry, VCH, Weinheim, 1996.
[35] A. De Meijere, S. Kozhushkov, T. Haumann, R. Boese, C. Puls, M.J. Cooney, L.T. Scott, Chem. Eur. J. 1 (1995) 124.
[36] L.T. Scott, M.J. Cooney, in: F. Diederich, P.J. Stang (Eds.), Modern Acetylene Chemistry, VCH, Weinheim, 1995, p. 347.
[37] R. Dierks, J.C. Armstrong, R. Boese, K.P.C. Vollhardt, Angew. Chem. Int. Ed. Engl. 25 (1986) 268.
[38] Y. Rubin, T.C. Parker, S.J. Pastor, S. Jalisatgi, C. Boulle, C.L. Wilkins, Angew. Chem. Int. Ed. Engl. 37 (1998) 1226.
[39] Y. Tobe, N. Nakagawa, K. Naemura, T. Wakabayashi, T. Shida, Y. Achiba, J. Am. Chem. Soc. 120 (1998) 4544.
[40] R. Boese, J.R. Green, J. Mittendorf, D.L. Mohler, K.P.C. Vollhardt, Angew. Chem. Int. Ed. Engl. 31 (1992) 1643.
[41] Y. Tobe, K. Kubota, K. Naemura, J. Org. Chem. 62 (1997) 3430.
[42] T.X. Neenan, G.M. Whitesides, J. Org. Chem. 53 (1988) 2489.
[43] N. Jux, K. Holczer, Y. Rubin, Angew. Chem. Int. Ed. Engl. 35 (1996) 1986.
[44] U.H.F. Bunz, V. Enkelmann, Angew. Chem. Int. Ed. Engl. 32 (1993) 1653.
[45] U.H.F. Bunz, V. Enkelmann, Organometallics 13 (1994) 3823.
[46] M. Altmann, V. Enkelmann, F. Beer, U.H.F. Bunz, Organometallics 15 (1996) 394.
[47] U.H.F. Bunz, V. Enkelmann, H.J. Räder, Organometallics 12 (1993) 4745.
[48] U.H.F. Bunz, G. Roidl, M. Altmann, V. Enkelmann, K.D. Shimizu, J. Am. Chem. Soc. 121 (1999) 10719.
[49] W. Steffen, M. Laskoski, G. Collins, U.H.F. Bunz, J. Organmomet. Chem. 630 (2001) 132.
[50] W. Steffen, M. Laskoski, J.G.M. Morton, U.H.F. Bunz, Organometallics, submitted.
[51] M. Laskoski, J.G.M. Morton, M.D. Smith, U.H.F. Bunz, J. Chem. Soc. Chem. Commun. (2001) 2590.
[52] M. Laskoski, J.G.M. Morton, M.D. Smith, U.H.F. Bunz, J. Organomet. Chem. 652 (2002) 21.
[53] M.S. Morton, J.P. Selegue, J. Organomet. Chem. 578 (1999) 133.
[54] Y. Rubin, C.B. Knobler, F. Diederich, Angew. Chem. Int. Ed. Engl. 30 (1991) 698.
[55] F. Diederich, Y. Rubin, Angew. Chem. Int. Ed. Engl. 31 (1992) 1101.
[56] R.M. Harrison, T. Brotin, B.C. Noll, J. Michl, Organometallics 16 (1997) 3401.
[57] K. Sonogashira, Y. Tohda, N. Hagihara, Tetrahedron Lett. 16 (1975) 4467.
[58] L. Cassar, J. Organomet. Chem. 93 (1975) 253.
[59] H.A. Dieck, R.F. Heck, J. Organomet. Chem. 93 (1975) 259.
[60] P. Nguyen, Y.A. Zheng, L. Agocs, G. Lesley, T.B. Marder, Inorg. Chim. Acta 220 (1994) 289.
[61] U.H.F. Bunz, Chem. Rev. 100 (2000) 1605.
[62] U.H.F. Bunz, in: D. Astruc (Ed.), Modern Arene Chemistry, Ch. 7, Wiley–VCH, Weinheim, 2002.
[63] S. Ohira, Synth. Commun. 19 (1989) 561.
[64] D.F. Taber, Y. Wang, J. Am. Chem. Soc. 119 (1997) 22.
[65] S. Müller, B. Liepold, G.J. Roth, H.J. Bestmann, Synlett 6 (1996) 521.
[66] D.G. Brown, E.J. Velthuisen, J.R. Commerfeld, R.G. Brisbois, T.R. Hoye, J. Org. Chem. 61 (1996) 2540.
[67] I.E. Marko, M. Tsukazaki, P.R. Giles, S.M. Brown, C.J. Urch, Angew. Chem. Int. Ed. Engl. 36 (1997) 2208.
[68] P.J. Garratt, K.P.C. Vollhardt, Aromatizität, Georg Thieme Verlag, Stuttgart, 1973.
[69] R. Faust, E.D. Glendening, A. Streitwieser, K.P.C. Vollhardt, J. Am. Chem. Soc. 114 (1992) 8263.
[70] R.H. Mitchell, Chem. Rev. 101 (2001) 1301.
[71] R.H. Mitchell, Y.S. Chan, N. Khalifa, P.Z. Zhou, J. Am. Chem. Soc. 120 (1998) 1785.
[72] J.M. Hunter, J.L. Fye, E.J. Roskamp, M.F. Jarrold, J. Phys. Chem. 98 (1994) 1810.
[73] R. Berscheid, F. Vögtle, Synthesis (1992) 58.
[74] M. Laskoski, W. Steffen, M.D. Smith, U.H.F. Bunz, J. Chem. Soc. Chem. Commun. (2001) 691.
[75] A.J. Boydston, M. Laskoski, U.H.F. Bunz, M.M. Haley, Synlett (2002) 981.
[76] M. Laskoski, M.D. Smith, J.M.G. Morton, U.H.F. Bunz, J. Org. Chem. 66 (2001) 5174.
[77] M. Laskoski, W. Steffen, J.G.M. Morton, M.D. Smith, U.H.F. Bunz, J. Am. Chem. Soc. 124 (2002) 13814.
[78] M. Laskoski, G. Roidl, M.D. Smith, U.H.F. Bunz, Angew. Chem. Int. Ed. Engl. 40 (2001) 1460.
[79] M. Laskoski, G. Roidl, H.L. Ricks, J.G.M. Morton, M.D. Smith, U.H.F. Bunz, J. Organomet. Chem. 673 (2003) 13.

[80] M. Laskoski, W. Steffen, J.G.M. Morton, M.D. Smith, U.H.F. Bunz, Angew. Chem. Int. Ed. Engl. 41 (2002) 2378.
[81] M. Laskoski, W. Steffen, J.G.M. Morton, M.D. Smith, U.H.F. Bunz, J. Organomet. Chem. 673 (2003) 25.
[82] S.M. Waybright, K. McAlpine, M.D. Smith, U.H.F. Bunz, J. Am. Chem. Soc. 124 (2002) 8661.
[83] A.J. Berresheim, M. Müller, K. Müllen, Chem. Rev. 99 (1999) 1747.
[84] M. Müller, C. Kübel, K. Müllen, Chem. Eur. J. 4 (1998) 2099.
[85] W. Steffen, B. Köhler, M. Altmann, U. Scherf, K. Stitzer, H.-C. zur Loye, U.H.F. Bunz, Chem. Eur. J. 7 (2001) 117.
[86] W. Steffen, U.H.F. Bunz, Macromolecules 33 (2000) 9518.
[87] M. Altmann, U.H.F. Bunz, Angew. Chem. Int. Ed. Engl. 34 (1995) 569.
[88] C.E. Halkyard, M.E. Rampey, L. Kloppenburg, S.L. Studer-Martinez, U.H.F. Bunz, Macromolecules 31 (1998) 8655.
[89] T. Miteva, L. Palmer, L. Kloppenburg, D. Neher, U.H.F. Bunz, Macromolecules 33 (2000) 652.
[90] J.N. Wilson, W. Steffen, T.G. McKenzie, G. Lieser, M. Oda, D. Neher, U.H.F. Bunz, J. Am. Chem. Soc. 124 (2002) 6830.
[91] B.M.W. Langeveld-Voss, D. Beljonne, Z. Shuai, R.A.J. Janssen, S.C.J. Meskers, E.W. Meijer, J.L. Bredas, Adv. Mater. 10 (1998) 1343.
[92] A.S. Davidov, Theory of Molecular Excitons, Plenum Press, New York, 1971.
[93] A.S. Davidov, Solutions in Molecular Systems, Kluwer, Amsterdam, 1991.